

AD-A146 674

CIRCULATION CONTROL APPLIED TO A HIGH SPEED HELICOPTER ROTOR

# DAVID W. TAYLOR NAVAL SHIP RESEARCH AND DEVELOPMENT CENTER

Bethesda, Md. 20884



CIRCULATION CONTROL APPLIED TO A  
HIGH SPEED HELICOPTER ROTOR

by

Kenneth R. Reader  
Joseph B. Wilkerson

DTIC  
ELECTE  
OCT 15 1984

B

APPROVED FOR PUBLIC RELEASE: DISTRIBUTION UNLIMITED

Reprint from the 32nd Annual National Forum of the  
American Helicopter Society, Washington, D.C.  
May 1976

DTIC FILE COPY

AVIATION AND SURFACE EFFECTS DEPARTMENT  
RESEARCH AND DEVELOPMENT REPORT

D. T. NSRDC

Report 77-0024

84-10-12-177



UNCLASSIFIED

SECURITY CLASSIFICATION OF THIS PAGE(When Data Entered)

(Block 20 continued)

➤ transition where high lift capability is needed while maintaining rotor moment trim. An analytical and experimental investigation of the aerodynamic environment in the transition flight regime (advance ratios of 0.5 to 1.4) indicates that large local yawed flow angles do not severely affect the lift augmentation and maximum lift coefficient of circulation control airfoils.

A RB-CCR model was designed and tested at the David W. Taylor Naval Ship Research and Development Center (DTNSRDC). This rotor is unique in its employment of a special circulation control airfoil which has a slot in the leading and trailing edge. The results of several test programs verified the capability of the rotor to perform efficiently in hover and at advance ratios up to 4.0. The model data also demonstrated that the rotor is capable of developing sufficient lift to fly through the critical advance ratio of 0.7.

DTIC  
ELECTE  
OCT 15 1984  
B

Accession For	
DTIC GRA&I	<input checked="" type="checkbox"/>
DTIC TAB	<input type="checkbox"/>
Unannounced	<input type="checkbox"/>
Justification	
By	
Distribution/	
Availability Codes	
Dist	Avail and/or Special
A-1	

DTIC  
COPY  
INTEGRATED

UNCLASSIFIED

SECURITY CLASSIFICATION OF THIS PAGE(When Data Entered)

## TABLE OF CONTENTS

	Page
ABSTRACT . . . . .	1
NOTATION . . . . .	1
SUBSCRIPTS . . . . .	1
SOLIDITY COMPROMISE . . . . .	2
LIFTING SYSTEM EFFICIENCY AND PARASITE DRAG . . . . .	3
RB-CCR MODEL . . . . .	4
ROTOR CONTROL REQUIREMENTS . . . . .	5
HOVER . . . . .	5
TRANSITION . . . . .	7
Aerodynamic Environment . . . . .	7
AZIMUTHAL PRESSURE SIGNAL PROGRAMMING EXPERIMENTS . . . . .	7
EFFECTS OF PRESSURE SIGNAL SCHEDULING . . . . .	9
REDUCED TIP SPEED (SCALE) EFFECTS . . . . .	9
COMPRESSOR POWER TRENDS IN TRANSITION . . . . .	10
RB-CCR THRUST CAPABILITY IN TRANSITION . . . . .	10
CRUISE . . . . .	12
SUMMARY . . . . .	13
REFERENCES . . . . .	13

## LIST OF FIGURES

1 - Effect of Simultaneous Leading and Trailing Edge Blowing . . . . .	2
2 - Dual Blowing Concept for Transition Advance Ratios . . . . .	2

	Page
3 – Thrust Generation Versus Speed . . . . .	3
4 – Variation of Power Required with $L/D_e$ and Flat Plate Area . . . . .	3
5 – RB-CCR Model Rotor Root and Tip Airfoil Profiles . . . . .	4
6 – RB-CCR Model in 8 x 10-Foot Wind Tunnel . . . . .	4
7 – RB-CCR Transition Control Requirements . . . . .	5
8 – RB-CCR Typical Control Signals . . . . .	5
9 – Reverse Blowing Circulation Control Rotor Hub . . . . .	6
10 – Leading Edge Slot and Solidity Effects in Hover . . . . .	6
11 – RB-CCR Hover Performance . . . . .	6
12 – Aerodynamic Environment . . . . .	7
13 – Sweep Angle Effects on a Circulation Control Fixed Wing . . . . .	8
14 – Pressure Signal Programming in Transition . . . . .	8
15 – Lift Offset For Controls Fixed . . . . .	9
16 – Tip Speed Effects in Transition . . . . .	10
17 – Power Trends in Transition . . . . .	10
18 – Maximum Thrust Capability . . . . .	11
19 – RB-CCR Model Characteristics in Transition with No Blowing . . . . .	11
20 – Power Tradeoffs in Cruise . . . . .	12
21 – Lift System Efficiency in Cruise . . . . .	12
22 – Thrust Level For Autorotation in Cruise . . . . .	13

---

Table 1 – Model Rotor Geometry . . . . .	4
--	---

## CIRCULATION CONTROL APPLIED TO A HIGH SPEED HELICOPTER ROTOR

Kenneth R. Reader  
Joseph B. Wilkerson  
David W. Taylor Naval Ship  
Research and Development Center  
Bethesda, Maryland 20084

### ABSTRACT

An advanced circulation control rotor concept identified as the Reverse Blowing - Circulation Control Rotor (RB-CCR) is discussed from the standpoint of general requirements for high speed flight. This discussion centers on a rotor solidity ratio compromise between hover, transition and cruise requirements. It is shown that the critical solidity requirement occurs in transition where high lift capability is needed while maintaining rotor moment trim. An analytical and experimental investigation of the aerodynamic environment in the transition flight regime (advance ratios of 0.5 to 1.4) indicates that large local yawed flow angles do not severely affect the lift augmentation and maximum lift coefficient of circulation control airfoils.

A RB-CCR model was designed and tested at the David W. Taylor Naval Ship Research and Development Center (DTNSRDC). This rotor is unique in its employment of a special circulation control airfoil which has a slot in the leading and trailing edge. The results of several test programs verified the capability of the rotor to perform efficiently in hover and at advance ratios up to 4.0. The model data also demonstrated that the rotor is capable of developing sufficient lift to fly through the critical advance ratio of 0.7.

### NOTATION

c	airfoil chord
$\bar{c}$	mean blade chord
$C_L$	lift coefficient
$C_m$	pitching moment coefficient, $\text{pitch}/\rho\pi R^3 V_T^2$
$C_P$	power coefficient, $P/\rho\pi R^2 V_T^3$
$C_T$	thrust coefficient, $T/\rho\pi R^2 V_T^2$
$C_L$	rolling moment coefficient, $\text{roll}/\rho\pi R^3 V_T^2$
$C_\mu$	blowing coefficient, $\dot{m} V_j/qc$
$\dot{m}$	mass flow rate, lbs/sec
N	number of blades
p	pressure, psig
q	freestream dynamic pressure, lbs/ft <sup>2</sup>
r	blade radial station, ft
R	rotor radius, ft
$V_j$	jet velocity, ft/sec
$V_T$	rotor tip velocity, ft/sec
X	non-dimensional radial station, r/R
$\alpha_s$	rotor shaft angle, deg
$\theta_c$	blade collection pitch angle, deg

$\Lambda$	local sweep angle, deg
$\mu$	rotor advance ratio, $V_\infty/\Omega R$
$\sigma$	rotor solidity ratio, $\sigma = N\bar{c}/\pi R$
$\psi$	rotor azimuth angle, deg (measured ccw from rear)

### SUBSCRIPTS

B	refers to blade
c	refers to compressor
H	refers to hub
j	refers to jet
T	refers to total or tip
w	refers to wing (fixed blade)
$\infty$	refers to free stream

The application of Circulation Control (CC) airfoils to helicopters was predicted by both the ability to increase  $C_L$  at a fixed angle of attack, and the ability to generate very high  $C_L$  without angle of attack stall. For typical angles of attack, circulation control airfoils demonstrate an ability to continually increase section  $C_L$  by blowing.

The concept of a Circulation Control Rotor (CCR) has been well established by industry studies and extensive wind tunnel evaluation at model scale. These results, and descriptions of the basic concept as applied to helicopters operating in the conventional speed regime, are well documented and may be found in references 1 thru 6.

In principle the concept involves a shaft-driven rotor with blades having circulation control airfoils. The CC airfoils employ a rounded trailing edge with a thin jet of air tangentially ejected from a slot adjacent to this (Coanda) surface. Airfoil lift is proportional to the momentum flux of this jet of air so that cyclic control requirements are obtained by cyclic modulation of the amount of blown air. The CCR requires an air supply duct within each blade and a continuous supply of compressed air. A simple throttling mechanism is used in the rotor head to provide control over both the cyclic and collective components of blown air, thus providing the cyclic and collective rotor control requirements. This process eliminates the need for blade cyclic pitch changes and may eliminate the collective pitch also. The rotor head is therefore free of numerous dynamic control system components thus greatly simplifying the mechanisms while presenting a cleaner profile from drag considerations. The subject of this paper is the extension of the above concept to a high speed, high advance ratio rotor system. Such a rotor concept has potential both as a reduced rpm, thrust compounded helicopter with speeds approaching 400 knots and as a stoppable rotor with speeds

approaching Mach 1.0 (reference 7).

As helicopter rotors approach higher speeds the problem of retreating blade stall is encountered due to the strongly reduced dynamic pressure and the relatively low maximum lift coefficient on classical airfoils. Because of this fundamental limitation, conventional rotors exhibit strongly reduced thrust capability (while maintaining trim conditions) as the advance ratio increases. Although several "fixes" to this problem have been forwarded (such as increased solidity ratio, auxiliary wings, contra-rotating rotors) the fact remains that such solutions result in increased weight, complexity and dynamical problems. The RB-CCR concept offers a radical departure from this dilemma. The Reverse Blowing - Circulation Control Rotor (RB-CCR) is a high speed variant of the CCR concept. It is so named because it makes use of double ended CC airfoils with both trailing edge and leading edge blowing. By simultaneous blowing from both slots on the retreating side of the disc, the airfoil is then capable of developing high positive  $C_q$  with the relative velocity coming from either direction (reverse or normal flow).

Two-dimensional airfoil experiments have shown it is possible to develop large lift coefficients by blowing from the appropriate individual slot or from both slots simultaneously. Typical two-dimensional data for this unique airfoil are shown in Figure 1 and are reported in detail in reference 8. Although some  $C_q$  reduction is evident with dual blowing, the high  $C_q$  capability still dominates. The advancing blade retains only trailing edge blowing because the relative velocity there is always in the conventional direction. This mode of operation, shown in Figure 2, allows the RB-CCR to maintain relatively high rotor thrust and trim capability in the transitional range ( $0.5 < \mu < 1.4$ ) where the retreating blade sees mixed flow conditions.

The operational regimes of a high speed rotor may be broken into three parts: conventional ( $\mu < 0.5$ ), transitional ( $0.5 < \mu < 1.4$ ), and cruise ( $\mu > 1.4$ ). In the conventional regime the RB-CCR uses only trailing edge blowing with normal one per revolution (1P) cyclic control. When the transition speed regime is reached, dual blowing is employed on the retreating blade and a two per revolution (2P) cosine control signal is added to provide additional lift on the fore and aft positions of the rotor disc. As speed is increased in transition the advancing blade tip Mach number approaches 0.9 and requires rotor rpm reduction to prevent drag divergence and to allow further speed increases. At approximately 250 knots ( $\mu = 0.7$ ) the rpm is reduced to 50-percent normal, while holding forward speed constant. This results in operation at  $\mu = 1.4$  and completes transition. From this point the rotor is considered to be in a cruise mode and may accelerate up to full forward speed. The cruise mode is characterized by the retreating blade being in a fully reversed flow field. Thus the blade "leading edge" is the aerodynamic trailing edge and only the leading edge blowing is used on the retreating side of the disc in cruise. Trailing edge blowing is still used on the advancing blade, resulting in an alternating blowing scheme: trailing edge for  $0^\circ < \psi < 180^\circ$ , leading edge for  $180^\circ < \psi < 360^\circ$ .

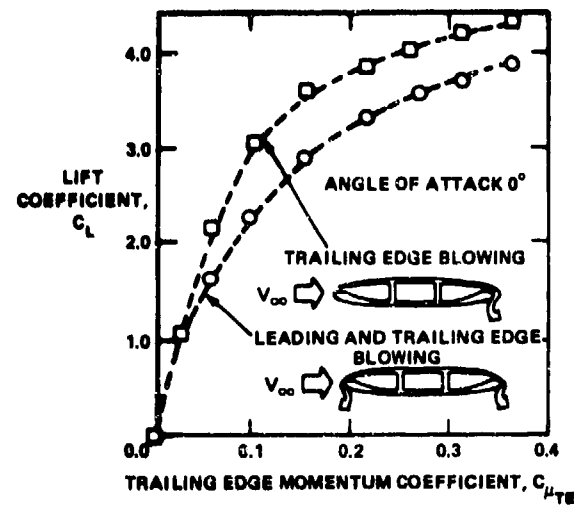


Figure 1 - Effect of Simultaneous Leading and Trailing Edge Blowing

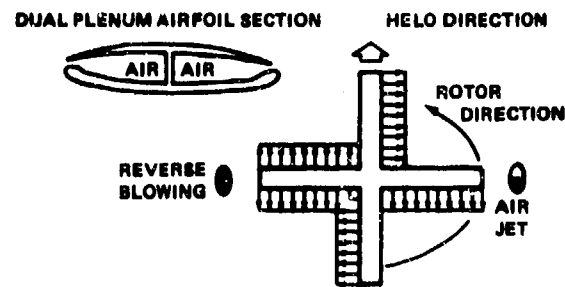


Figure 2 - Dual Blowing Concept for Transition Advance Ratios

The basis for this sequence of conditions was first reported in reference 9 and has been retained pending analysis of more definitive model rotor data.

#### SOLIDITY COMPROMISE

The most significant single factor affecting performance of a high speed lifting rotor concept is the design compromise in solidity to bring about satisfactory lift and controlability in transition without over penalizing the cruise speed and efficiency. Near the 0.7 advance ratio condition the blade loading capability on the retreating side becomes a minimum, thereby reducing the rotor thrust which can be developed while maintaining roll trim conditions. Since blade loading is the key to this problem, one solution would be to increase the blade area, or solidity ratio. At cruise conditions (advance ratios greater than 1.4) the blade loading capability is quite good. Here, increased solidity would force the airfoils to work at  $C_q$  conditions far below the optimum, while adding considerable skin friction drag due to the increased area. Consequently a solidity compromise allows neither transition nor cruise conditions to be effectively designed to.

The RB-CCR system must have a solidity compromise too, but to a much lesser extent than concepts using conventional airfoils. It uses the higher section  $C_q$  obtainable from circulation control airfoils to boost blade loading capability during transition. This allows a higher  $C_T/\sigma$  in transition without the penalizing effects of higher solidity in cruise. The RB-CCR model thrust capability is shown in Figure 3 for the transition speed range using dual blowing on the retreating blade and both a 1P and a 2P cyclic control input. This thrust generating ability far exceeds that of other systems for equal solidity (directly related to blade weight) and at a zero shaft angle. Somewhat higher values are expected with operation at positive shaft inclinations.

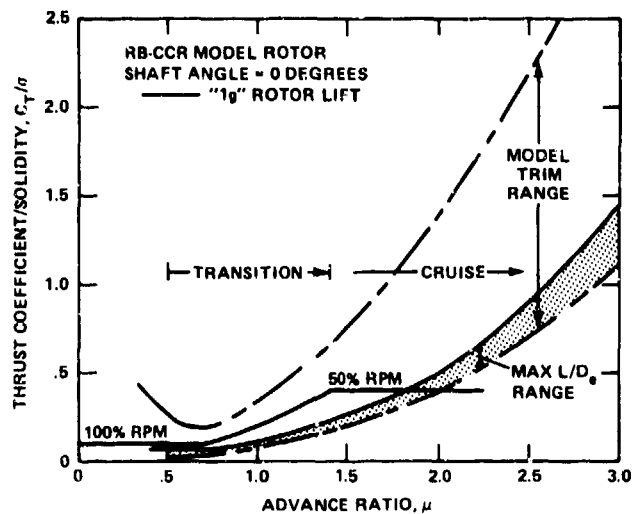


Figure 3 - Thrust Generation Versus Speed

#### LIFTING SYSTEM EFFICIENCY AND PARASITE DRAG

The overall efficiency tradeoff must be considered across the range of advance ratio. Model rotor data have established the  $C_T/\sigma$  for best lifting system efficiency and have identified a basic operational  $C_T/\sigma$  range for the condition of zero shaft angle. Figure 3 shows these variations in comparison to the intended  $C_T/\sigma$  schedule for 1g operation. As rotor rpm is reduced the  $C_T/\sigma$  must increase to maintain 1g loads: a 50-percent reduction in  $V_T$  requiring a four fold increase in  $C_T/\sigma$ . It is desirable to operate as close as possible to the region of maximum efficiency. The selection of a design operating condition must be weighted by the relative importance of each speed regime and by considerations of power sharing between rotor power and the auxiliary propulsive power. It should be noted however that this selection cannot be completed until additional data are available over an appropriate range of rotor shaft angles.

The lifting system  $L/D_e$  (beyond approximately 10.0) in high speed cruise flight has been shown to be much less important than the vehicle equivalent flat plate drag area (reference 9).

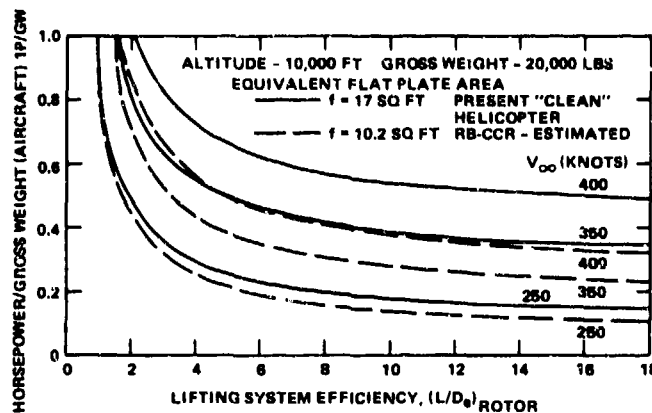


Figure 4 - Variation of Power Required with  $L/D_e$  and Flat Plate Area

Figure 4 for example shows that the vehicle total horsepower to gross weight requirement in cruise is much more sensitive to a 40 percent reduction in flat plate area than it is to an improvement of even 100 percent in lifting system efficiency. The flat plate area of  $f = 17$  sq. ft. for a vehicle of  $GW = 20,000$  lbs. would be considered quite clean by present standards of helicopter drag levels, but that is almost three times the drag of a fixed wing aircraft for the same gross weight. It may be concluded from this, and indeed was concluded by the 1975 AHS Ad Hoc Committee on Rotorcraft Parasite Drag, that considerable improvements can and should be made and that a 40-percent drag reduction is not unreasonable for conventional rotor system. The RB-CCR design lends itself to extremely low drag hub designs, and should produce at least this much reduction in total drag. Reference 10 presents large scale data of such a "clean" design.

As previously mentioned, a proper balance must be struck between the power requirements (efficiency) for transition and those for cruise. By far the majority of power required in cruise is demanded from the auxiliary propulsion to overcome vehicle parasite drag (which includes hub drags). Transitional power required, however, is shared between rotor power (shaft plus compressor for the RB-CCR) and the auxiliary propulsion power. An important question for a proper power balance is "What lifting system efficiencies are required in transition and in cruise flight?". Referring back to Figure 4, it appears that for cruise at 400 knots a lifting system  $L/D_e$  of 12 to 14 is most reasonable. If the total power in transition at 250 knots were no greater, then a lifting system  $L/D_e$  of about 2.6 would produce a power balance. Certainly, it would appear that a lifting system  $L/D_e$  of 3 to 4 in transition would be more than compatible with the expected reduced drag levels for cruise. In concept then, the requirements for rotary wing lifting system efficiency are not really very demanding. The RB-CCR model rotor has in fact demonstrated these requirements for a zero shaft angle setting, and future evaluation at positive shaft angle settings promise additional improvements.

## RB-CCR MODEL

Analytical studies of the RB-CCR concept have established a baseline rotor design in terms of operational  $C_T/\sigma$ , blade twist and airfoil distributions of thickness and camber. Also included in these studies were the effects of 2P content in the pneumatic cyclic control signal. The resulting RB-CCR configuration was designed and manufactured at DTNSRDC as an 80-inch diameter four-bladed rotor model to be evaluated in the 8 x 10-Foot North Subsonic Wind Tunnel of the Aviation and Surface Effects Department.<sup>1</sup> The airfoil sections were symmetrical about the mid chord with both a leading edge slot and a trailing edge slot. Thickness distribution varied linearly from 20-percent at the root to 15-percent at the tip; camber distribution varied from 5-percent at the root to zero at the tip. The inboard airfoil was chosen for its high  $C_q$  capability and excellent blowing augmentation ratio (high efficiency). It enables the retreating blade to develop higher lift in the low dynamic pressure field of reversed flow. The tip airfoil was designed to have good critical Mach number characteristics for advancing blade operation and to still exhibit good augmentation characteristics for retreating blade operation. The root and tip CC airfoil profiles are shown in Figure 5.

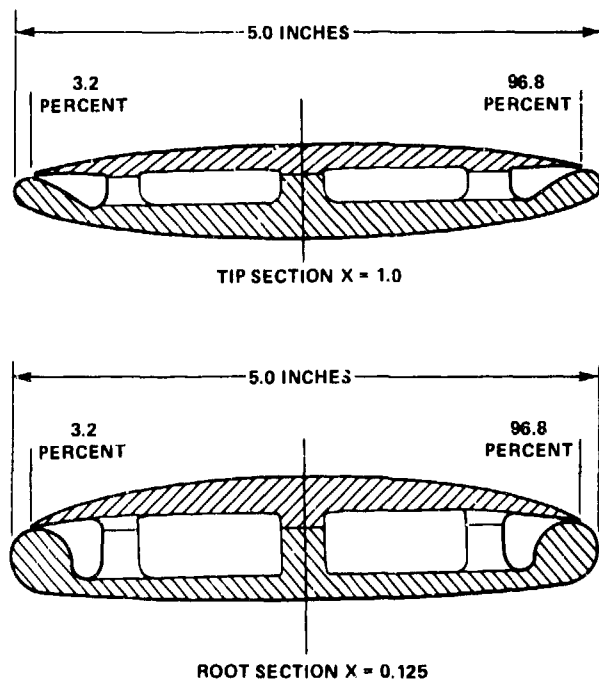


Figure 5 - RB-CCR Model Rotor Root and Tip Airfoil Profiles

Slot positions were a constant percentage of chord over the blade radius:  $x/c = 0.032$  leading edge and  $x/c = 0.968$  trailing edge. The slot height to chord ratio was also constant  $h/c = 0.002$  for both leading and trailing edge slots. Each slot was supplied air from a separate duct within the blade so that blowing from either the leading edge slot or the trailing edge slot could be independently controlled (see Figure 5). The mechanism for controlling the air supply was located inside the model head and will be explained in a subsequent section.

The blades were machined from solid aluminum alloy in upper and lower halves by numerically controlled machines. Internal duct geometry and the slot regulating posts were cut at the same time to insure equal mass and stiffness distributions between the blades.

The physical characteristics of the model are summarized in Table 1. Figure 6 shows the RB-CCR in the wind tunnel. It should be noted that the model solidity ratio is considerably larger than that which was designed or required for a full scale RB-CCR.

TABLE I  
Model Rotor Geometry

BLADE	RB-CCR
DIAMETER, FT	6.67
NUMBER OF BLADES	4
CHORD, IN.	5
SOLIDITY RATIO	0.1592
GEOMETRIC TWIST, DEG.	0
AIRFOIL	ROOT/TIP
THICKNESS RATIO, $t/c$	0.20/0.15
CAMBER RATIO, $\delta/c$	0.05/0.0
TRAILING EDGE RADIUS, $R_{TE}/C$	0.052/0.022
SLOT HEIGHT RATIO, $h/c$	0.002/0.002



Figure 6 - RB-CCR Model in 8 x 10-Foot Wind Tunnel

<sup>1</sup>This work was conducted under the sponsorship of the Naval Air Systems Command. The analytical study was performed, among others, by Mr. E.O. Rogers at DTNSRDC.

The scaled chord for the correct solidity would have resulted in a model chord of 2.8 inches and a slot height of 0.0056 inches. The requirement of two slots per blade (and two air supply ducts per blade) made this small chord very impractical from a manufacturing point of view. Therefore the chord was arbitrarily increased to 5 inches, allowing a slot height of 0.010 inches. It was also realized that this would increase loads and provide more accurate data at the reduced tip speeds corresponding to model operation at high advance ratio. Basically this step gave the model blades a lower aspect ratio than the full scale design, so that the model data at full scale  $C_T/\sigma$  should be somewhat pessimistic in both thrust ability and power required.

The RB-CCR model data has established baseline characteristics for the high speed CCR concept from hover through transition and into cruise to advance ratios of 4.0. It was necessary to run the model at tip speeds below those intended for full scale at the higher advance ratio range. While this did not allow Mach number scaling, the data are scaled for  $C_T/\sigma$  which accounts for the reduced tip speed and increased solidity. The data presented in later sections are strictly model data, they have not been corrected to full scale Mach number or full scale Reynolds number. All data points represent a fully trimmed condition (shaft roll moment and pitch moment trimmed to zero by cyclic control) at the thrust level  $C_T/\sigma$  indicated unless otherwise noted. All of the data shown were taken at a shaft inclination angle of zero degrees.

#### ROTOR CONTROL REQUIREMENTS

The basic control concept was alluded to earlier in the paper. This discussion will center upon three distinct flight regimes and the type of pneumatic control required. Three flight regimes were defined: low advance ratio ( $0 < \mu < 0.5$ ), transitional advance ratio ( $0.5 \leq \mu \leq 1.4$ ), and high advance ratio ( $\mu > 1.4$ ). In the low advance ratio range, only the trailing edge duct was blown and the pressure wave was basically a 1P sine wave. In the transitional range, the trailing edge duct was blown from 0 to 360 degrees azimuth and the leading edge duct from approximately 180 to 360 degrees (0 degree being at the rear of the rotor disc). In the dual-blowing region of the disc (retreating side) the pressure waves in both ducts was the same; the addition of a 2P pressure component to the basic 1P has been shown to be beneficial for this portion of the flight regime (Figure 7). At high advance ratios, the trailing edge duct was blown from 0 to 180 degrees and the leading edge duct from 180 to 360 degrees. The pressure wave was basically a 1P sine wave in both ducts, with minimum blowing occurring within 0 to 180 degrees and maximum blowing within 180 to 360 degrees. Typical pressure control signals that are produced by the cams of the RB-CCR model have various amounts of 2P (Figure 8).

The valving system of the RB-CCR azimuthally programs the airflow to the leading edge slot, to the trailing edge slot, or to both slots of a dual-slotted rotor blade. The system still retains a cam-nozzle relationship (similar to those used in previous CCR models) to provide the airflow harmonic content necessary to control the rotor. A detailed discussion of the

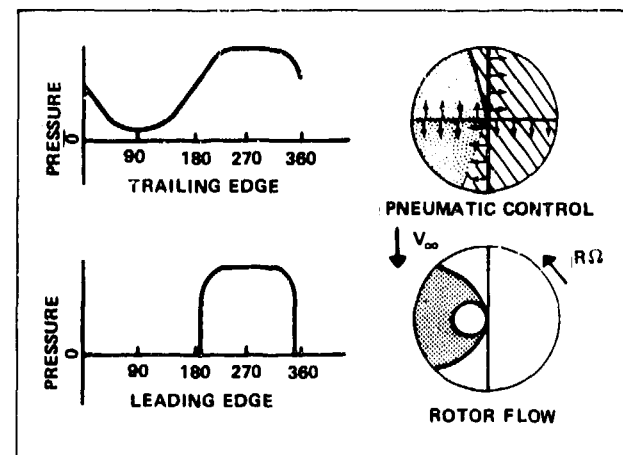


Figure 7 - RB-CCR Transition Control Requirements

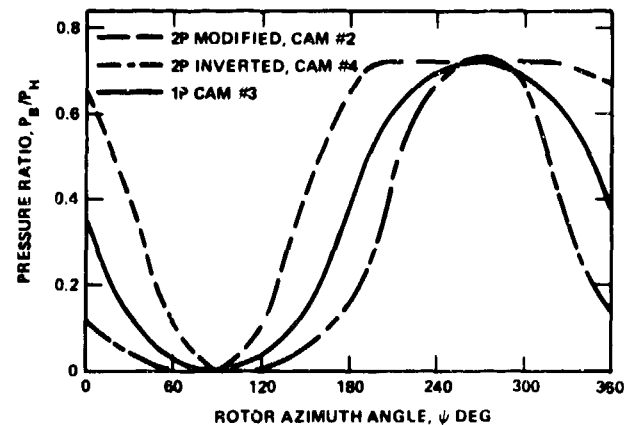


Figure 8 - RB-CCR Typical Control Signals

RB-CCR valving system is presented in reference 11. Figure 9 shows the control system used for the wind tunnel model.

#### HOVER

Basic hover performance of the RB-CCR was obtained over a thrust range for different tip speeds, collective pitch angle, number of blades and blade leading edge condition. Although the RB-CCR was designed for performance at an advance ratio of 0.7, it proved to have good efficiency in the hover mode. The improved airfoil trailing edge design of this rotor demonstrated reduced compressibility effects relative to those reported in reference 4. At high tip Mach number the rotor thrust augmentation was not adversely affected and profile power showed only a slight increase.

The rotor was evaluated in hover as both a two-bladed and a four-bladed rotor with corresponding solidities of 0.0796 and 0.1592. It was anticipated that the leading edge slot could cause

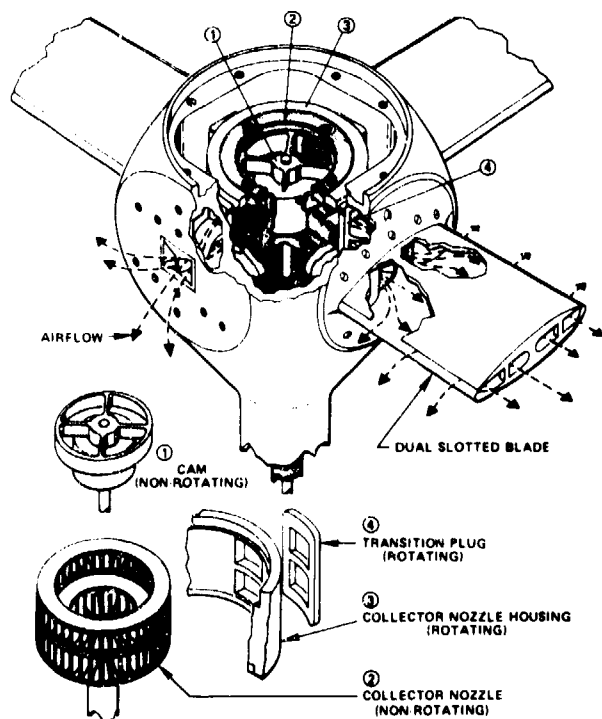


Figure 9 - Reverse Blowing Circulation Control Rotor Hub

a power penalty, so the two-bladed configuration was evaluated with the leading edge slot both open and covered. Radial covering was effected by taping over the slot, thus providing a smooth aerodynamic shape to local flow in that region of the airfoil. An increase in total power was noted with the leading edge slot open. Figure 10 shows the power increase at the lower thrust coefficients was due to an increase in shaft power and at the higher thrust coefficients was due to an increase in compressor power. This power increase, due to the open leading edge slot, gave a corresponding reduction in hover Figure of Merit relative to the covered configuration. The reduction in hover Figure of Merit dictates that some means of concealing the leading edge slot (when not in use) be incorporated into a full scale rotor. One suggested means might be a flexible slot lip.

The four-bladed rotor was tested only with the leading edge slot exposed and shows performance equal to the exposed slot data from the two-bladed rotor; see Figure 11. This agreement in hover Figure of Merit with the leading edge slots open suggests that the four-bladed rotor would have a much improved Figure of Merit with the slots covered (similar to the two-bladed performance with covered slots at the same  $C_T/\sigma$ ). Figure 11 also shows the tendency to maintain a level of hover efficiency over a broad  $C_T/\sigma$  range, even for the constant collective pitch setting shown. This is a basic characteristic of the RB-CCR model and of prior CCR model rotors. The maximum thrust obtained for the four-bladed rotor does not represent aerodynamic limitations. It was limited by the hydraulic power unit used

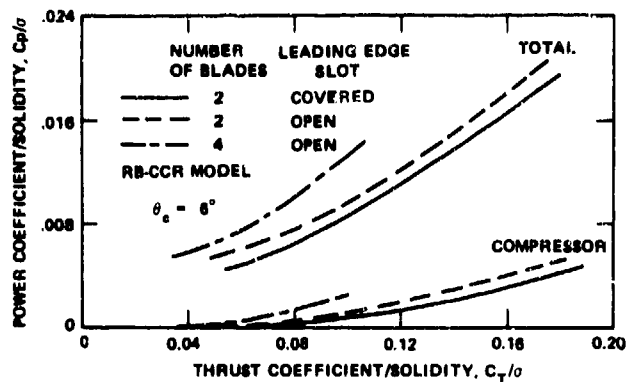


Figure 10 - Leading Edge Slot and Solidity Effects in Hover

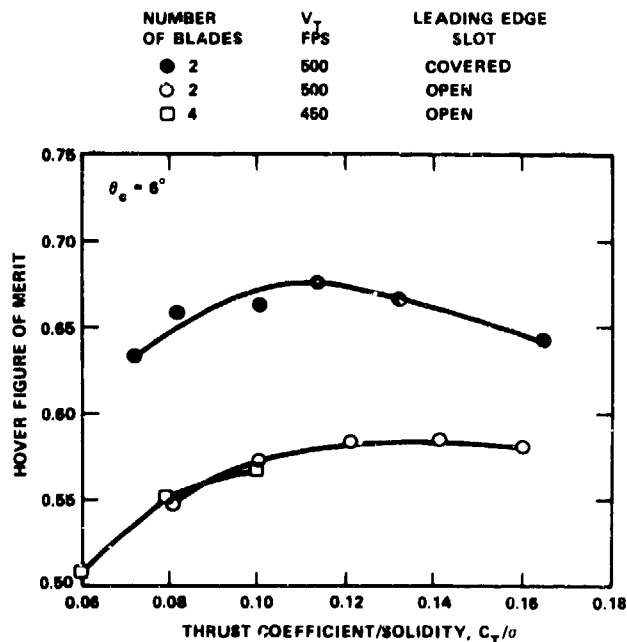


Figure 11 - RB-CCR Hover Performance

to provide rotor shaft power. The highest  $C_T/\sigma$  shown for the four-bladed rotor is at about the same disc loading as the highest  $C_T/\sigma$  shown for the two-bladed rotor. The two end points therefore represent about the same shaft torque requirement.

Good Figure of Merit can be obtained over a large range of collective pitch angles. A comparison of configurations at various collective angles showed a steady performance improvement with increasing collective pitch angle (up to  $\theta_c \approx 6^\circ$ ). Although operation with zero collective was indeed possible at a Figure of Merit of about 0.50.

The peak Figure of Merit obtained in this test was 0.68 at a  $C_T/\sigma = 0.114$ . When considered in light of strong adverse model scale Reynolds number effects, the low aspect ratio per blade of only 8.6 and a simple squared tip shape the results are basically conservative. Furthermore the rotor is untwisted with constant slot height. It would then appear that optimization of these parameters may potentially increase maximum Figure of Merit beyond those of today's best rotors, and at higher  $C_T/\sigma$  design values.

## TRANSITION

### Aerodynamic Environment

The reduced thrust capability of a rotor system at  $\mu = 0.7$  is in fact due to more than simply the reduced dynamic pressure on the retreating blade. Two other factors also play an important role on the retreating side of the disc: angle of attack and flow yaw angle. Figure 12 indicates their variation with blade radius for three azimuth positions. The conditions are zero shaft angle and 0.7 advance ratio. Uniform inflow is assumed. The variation of dynamic pressure, angle of attack, and yaw angle applies to any rotor system in this flight condition, as it simply describes the relative magnitude and orientation of the resultant velocity vector to the blade element. Also shown is the radial variation of  $C_q$  for each azimuth position as currently predicted for the RB-CCR in trimmed flight.

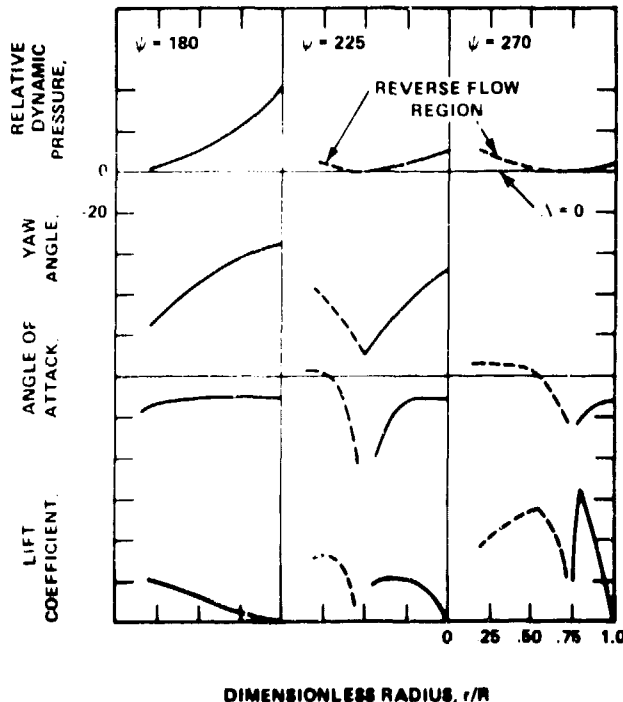


Figure 12 - Aerodynamic Environment  
( $\alpha_s = 0$ ,  $\mu = 0.7$ ,  $C_q$  For  $C_T/\sigma = 0.10$ ,  $\alpha$  For  $\theta_c = -4.0^\circ$ )

At  $\psi = 180^\circ$  the inboard yaw angles are seen to be quite large, but the angle of attack is moderate and  $C_q$  demands are not large in comparison to CC airfoil capabilities. At  $\psi = 225^\circ$  the relative dynamic pressure has dropped considerably (being zero at  $r/R = 0.5$ ) and yaw angles have become more severe. The section angles of attack approach  $-90$  degrees at  $r/R = 0.5$ . At other radial stations the  $C_q$  requirement has increased to 2.0 or 3.0. While this is within the capability of CC airfoils, it naturally requires a higher  $C_\mu$  to overcome the large negative angles and the effects of extreme yaw angles. Finally at  $\psi = 270^\circ$  the relative dynamic pressure reaches a minimum. More importantly, the dynamic pressure is quite small over the outer 50-percent of the blade. This coupled with significant negative angles of attack over the outer 40-percent of the blade, severely reduce the ability of the blade to generate hub moments even though it can still carry an appreciable inboard lift.

As an over simplification, one may argue that the blade center of lift is at the 75-percent radius. Then retreating blade lift and moment generation would go to minimum values as local  $q$  approached zero at that radius. This condition occurs at  $\mu = 0.75$  for a zero shaft angle, which agrees quite well with the advance ratio for minimum thrust for both model data and predicted values.

Some information has been obtained on the effects of yaw angle on CC airfoil performance. The data were taken from a half wing over a range of sweep angles. While the data do not represent 2-D yawed flow, the characteristic wing performance must reflect the effects of yawed flow on the airfoil sections. Consequently, the data are considered to be at least representative of yaw effects. Figure 13 shows the wing data for different sweep angles across a  $C_{\mu_w}$  range, as reduced relative to the chordwise direction (lift and momentum flux are normalized by the area times the dynamic pressure perpendicular to the blade span axis). It can be noted that the "lift augmentation" ( $\Delta C_L / \Delta C_{\mu_w}$ ) is essentially unaffected by yaw angle until  $\Lambda > 45^\circ$ . Similarly the maximum wing  $C_L$  capability is not adversely affected, even to extreme yaw angles. Although the data are not strictly two-dimensional, it suggests a very mild influence of yaw angle on either augmentation or maximum lift for moderate yaw angles.

### AZIMUTHAL PRESSURE SIGNAL PROGRAMMING EXPERIMENTS

A large portion of the wind tunnel evaluation was dedicated to experimentally determining ways to reduce the compressor power in the transition flight regime. Notwithstanding the strong Reynolds effects discussed later it was felt that azimuthal blowing schemes might be optimized to minimize the compressor requirement. The azimuth blowing schemes were set up by physically blocking the collector nozzle so that the blades only received air over a chosen range of azimuth. Small regional changes of dual blowing on the retreating side of the rotor showed no detrimental effect on the rotor efficiency. However when the trailing edge slot is restricted from blowing over an azimuth range of 15 to 180 degrees there is a moderate increase in compressor power.

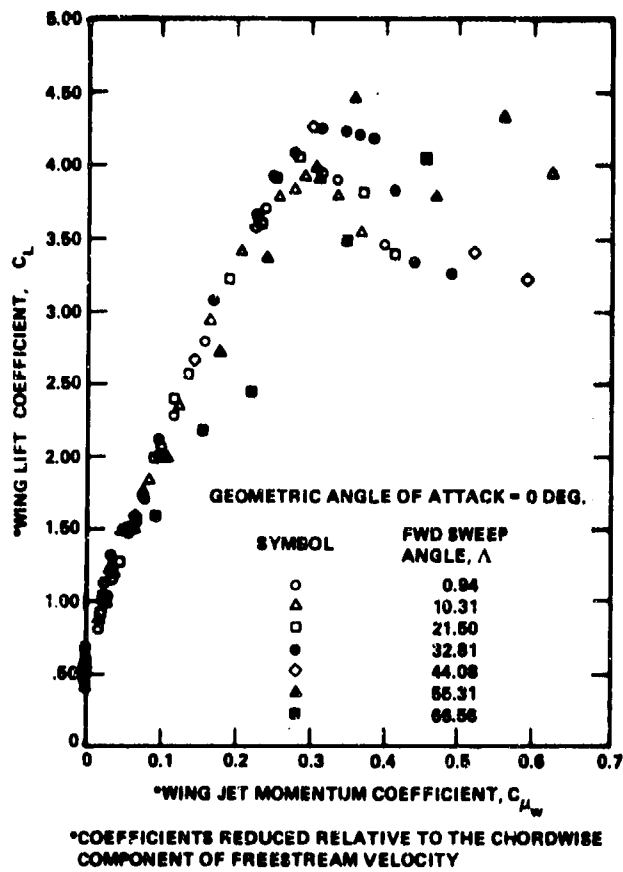


Figure 13 - Sweep Angle Effects on a Circulation Control Fixed Wing

Radial covering of the slots was also studied by spanwise taping over selected portions of the slots. The blades were radially taped, as determined by the reverse flow circle on the retreating side of the rotor, to take advantage of minimizing the mass flow and the leading edge slot effects. While the spanwise variation in blowing was primarily to minimize blowing on the retreating side of the rotor (where blowing is a maximum) it also restricted a large portion of the trailing edge slot on the advancing side of the rotor (where blowing is a minimum). To realize the maximum effect only the leading edge slot as determined by the local flow direction should be covered. The reverse flow circle for advance ratios of 0.5 and 0.7 were used to determine the portion of the leading and trailing edge slots to be covered. For the advance ratio of 0.5 (0.7) the trailing edge slots of all the blades were covered for the inboard 50 (70)-percent and the leading edge slot of all the blades were covered for the outboard 50 (30)-percent. (The numbers in parenthesis are for an advance ratio of 0.7). While both of these configurations show reductions in compressor power, the advance ratio of 0.5 configuration showed a significant improvement over the advance ratio of 0.7 configuration and will be discussed below (Figure 14). For the advance ratio of 0.5 configuration it was noted that the rotor required only half as much blade pressure at a  $C_T/\sigma$  of 0.04 as for the uncovered

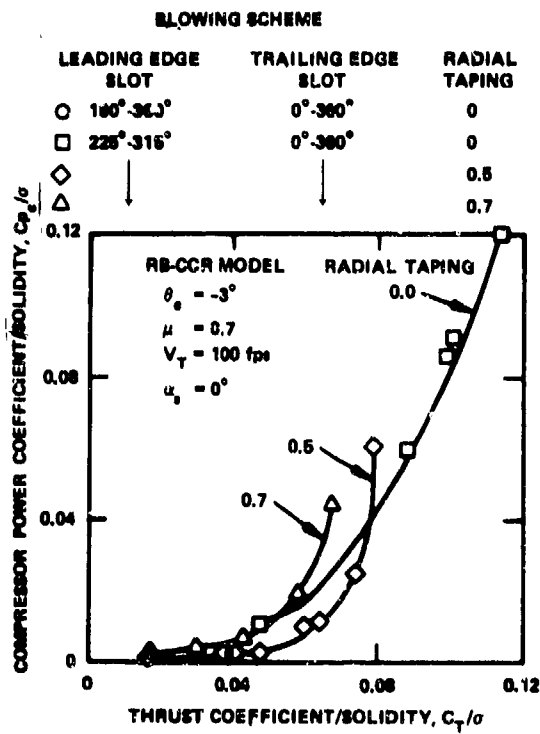


Figure 14 - Pressure Signal Programming in Transition

configuration. Analysis of the rotor data indicated that the reduced pressure was due to improved blowing augmentation with a subsequent improvement of approximately 50-percent in compressor power. A 50-percent reduction in shaft power was also observed. A full analysis of the rotor is not complete; the above observations are presented to show the potential gain that are available from this concept.

The azimuthal programming requirement to most efficiently control the rotor was investigated by varying the rotor azimuthal blowing schedule and also varying the region of the rotor over which dual blowing, single blowing and no blowing was available. The various programming schemes are presented as an insert in Figure 15. The state variables which were fixed throughout the programming schemes are: cam configuration;  $V_T = 100$  fps;  $\theta_c = 0^\circ$ ;  $\mu = 0.7$ ; and  $\alpha_s = 0^\circ$ . The data were obtained by setting the tunnel conditions; then recording data at zero blowing and for increasing amounts of blowing while the controls were fixed for maximum roll control (100-percent cam and maximum blade pressure at  $\psi = 270^\circ$ ). Attempts were then made to trim the rotor model in pitch and roll moment for some thrust level. With no blowing on the advancing side of the rotor and a zero collective pitch angle, the trimmed thrust capability is very restricted and requires a delicate balance between the amount of thrust generated and the distribution of this thrust. When there is no blowing on the advancing side of the rotor and the control pressure signal distribution is fixed, the rotor will trim at only one thrust level for each collective pitch angle.

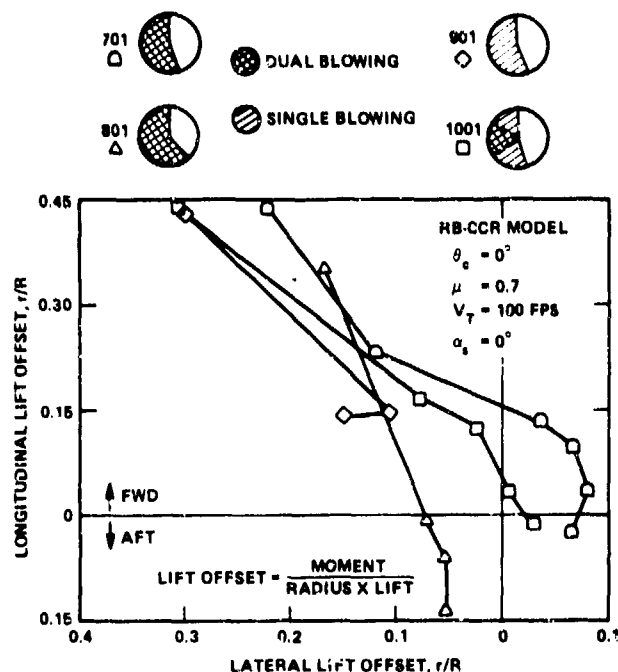


Figure 15 - Lift Offset For Controls Fixed

The non-dimensional lift center of pressure for the various configurations with the controls fixed is presented in Figure 15. (For clarification, the configuration number will be referenced in parenthesis). When only trailing edge blowing was used on the retreating side of the rotor and no blowing was used on the advancing side (Configuration 901) the rotor was untrimmable in both roll and pitch moment. Dual blowing (simultaneous blowing of both leading and trailing edge) over the same region showed that the rotor could be trimmed in both roll and pitch moment, verifying that dual blowing is required for trim at 0.7 advance ratio (Configuration 701). As blowing was increased the curve for Configuration 701 showed that too much roll control was available with the phase angle of maximum blowing at 270 degrees and that total trim could be obtained by rotating the position of maximum blowing into the fourth quadrant of the rotor and reducing the blade pressure. This is, in fact, what was required to fully trim the rotor for this configuration. The region of dual blowing was then reduced to a 60-degree wedge extending from an azimuth of 240 to 300 degrees (Configuration 1001). This configuration represents a blowing scheme that almost gives roll and pitch trim control although at a higher blade pressure for the same thrust. The effectiveness of generating lift on the aft portion of the disc ( $15^\circ < \psi < 45^\circ$ ) was determined by extending the dual blowing region from 15 to 45 degrees on the aft portion of the disc (Configuration 801). For this configuration the rotor could be pitch trimmed very easily but could not be roll trimmed. The effectiveness of the rotor to generate lift in the  $15^\circ < \psi < 45^\circ$  region is adequate to keep the rotor from being trimmed with the controls fixed for maximum roll control. To fully trim the rotor the cam had to be rotated approximately 56 degrees into the third quadrant. This

essentially removed all the blowing from the aft region ( $0^\circ < \psi < 45^\circ$ ) of the rotor. It is concluded that the rotor can develop substantial amounts of lift on the fore and aft portions of the disc.

#### EFFECTS OF PRESSURE SIGNAL SCHEDULING

The RB-CCR wind tunnel evaluation demonstrated the ability of the rotor to fly through transition at relatively high  $C_T/\sigma$  ratios. A fully trimmed  $C_T/\sigma$  of 0.24 was achieved at the critical advance ratio of 0.7; a  $C_T/\sigma$  of 0.62 was generated at an advance ratio of 1.4. Neither limit was aerodynamic in nature but were produced by model blade pressure restrictions, cam shape limits, or balance frame vibrations.

The compressor power of the rotor can be reduced by lowering the pressure required to achieve a given thrust level. Near minimum compressor power the rotor performance is especially sensitive to blade collective pitch. Historically, CC Rotors have been limited in rotor thrust levels not by  $C_q$  capability, but by trim requirements. The disparity in velocities and angles of attack of the advancing blade and retreating blade are the prime cause for trim problems. However, proper scheduling of the blowing can accommodate these differences. The amount of blowing occurring at any point on the disc on the wind tunnel model is controlled by the shape of the particular control cam. Therefore, the rotor trim capability can be improved by judiciously designing the control cam to provide more appropriate pressure waves to the rotor blades with the model. (In a full scale rotor the fixed cam is replaced by a fully variable control valve to give an arbitrary signal).

The model rotor control requirements vary with rotor thrust levels. Low  $C_T/\sigma$ 's or low hub pressures require pitch control input almost entirely. As thrust levels are increased by blowing the inability of a fixed cam to restrict the amount of air being blown on the advancing side of the disc results in roll control limits. Both of these control requirements become even more stringent when collective angle is increased. To improve the understanding of the rotor system control scheduling and to reduce compressor powers through transition, five cams which produce different pressure scheduling were evaluated. The cams produced significant increases in rotor moment capability while also reducing compressor power.

#### REDUCED TIP SPEED (SCALE) EFFECTS

The model rotor had to be tested at reduced tip speed for advance ratios greater than 0.5. The limiting factors in selecting a tip speed for the model rotor were natural frequency excitations, tunnel maximum speed and advance ratio. A practical speed limit of the tunnel is 200 fps. The operational limits of the model rotor were established by  $\mu \times V_T \leq 200 \text{ fps}$ . The rpm which corresponds to blade natural frequency and multiples of this frequency had to be avoided to keep from exciting the wind tunnel balance and to keep blade bending moments within structural limits. The rotor was operated with selected control system configurations for the same advance ratio but at different tip speeds, to determine the effect of tip speed on the model

performance. The largest effect of increasing tip speed is to correspondingly increase the Reynolds number at which the blade sections are operating. (Due to reduced tip speed and model size there is approximately a factor of 20 between model and full scale rotor Reynolds number). The tendency of the model rotor to perform better at higher Reynolds number is consistent with the type of two-dimensional Reynolds number corrections that have been applied in correlating previous model rotors to the rotor performance program. As discussed previously the retreating side of the rotor is in a very low velocity and Reynolds number region; the effects of increasing the tip speed are shown in Figure 16 for advance ratio of 0.7.

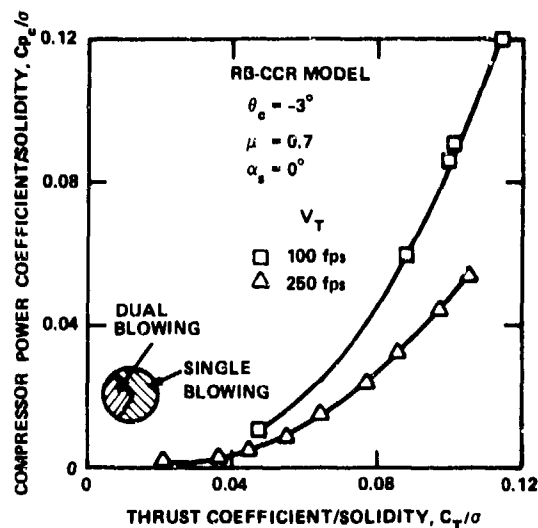


Figure 16 - Tip Speed Effects in Transition

An increase in tip speed increases the blade profile power which reflects a very small increase in shaft power at an advance ratio of 0.5 and negligible effects at an advance ratio of 0.7. The induced power will not be the same for both tip speeds. The increase in performance is provided by much better CC augmentation which is manifested in a substantial reduction in compressor power. The ratio of compressor power to total power shows that much less compressor power is required at the high tip speed. The ratio of compressor power to total power has shown a consistent reduction with increasing tip speed for the data analyzed to date.

It is quite evident from these results that Reynolds number effects are very significant. While rotor parameter trends are probably represented reasonably well by the data, an attempt to arbitrarily extrapolate to full scale without a thorough knowledge of the scaling laws would be very questionable. This is particularly true with regard to profile and compressor power due to their strong dependence on the boundary layer momentum thickness, and hence Reynolds number.

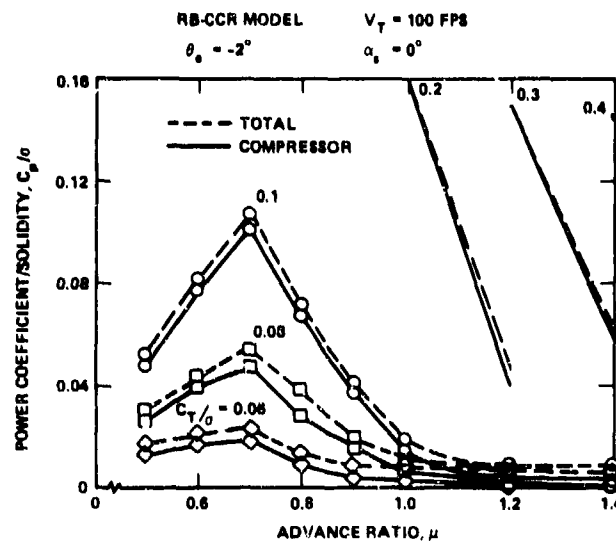


Figure 17 - Power Trends in Transition

#### COMPRESSOR POWER TRENDS IN TRANSITION

The trends of the compressor power for the transition flight are presented in Figure 17 for the rotor alone. The data are for a tip speed of 100 fps. The trends of the data are of primary importance and not the absolute magnitude of the data (due to the Reynolds effects, discussed above). At the critical advance ratio of 0.7, 80 to 90-percent of the power required is from the compressor. In effect the rotor is nearing autorotation (shaft power approaching zero) at these conditions. Note that zero shaft angle was the only condition studied. At lower and higher advance ratios the compressor requirement rapidly diminishes (see section on cruise performance) so that the 0.7 condition actually "sizes" the compressor installed. (In an actual aircraft the compressor power is extracted on the high rpm engine shaft before the main transmission. This approach permits the desired power sharing).

#### RB-CCR THRUST CAPABILITY IN TRANSITION

The major question to be answered by this model investigation was "can the RB-CCR generate full lift thru transition?". Due to the complexity of the 0.7 advance ratio flow environment the prediction method (reference 7 and 9) required some unsubstantiated assumptions. The experimental answer is a definite yes and substantiating data are present in Figure 18. This figure presents the range of fully trimmed thrust condition established by the model rotor. The boundaries of the data are actually established by model limits and not fundamental aerodynamic ones. The lower boundary is restricted by the minimum thrust at which the model can be trimmed and is characterized by low blowing rates and minimum power. The upper boundary is restricted by particular limits placed on the model rotor design. Examples of these limits are blade loads, blade internal pressure, balance-model vibrations and most importantly rotor trim limits at high lift conditions.

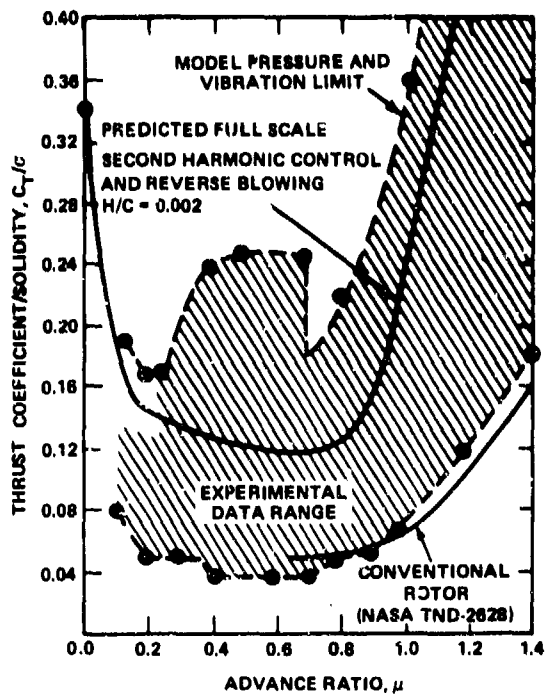


Figure 18 - Maximum Thrust Capability

A full discussion of the trim limits of CC rotors is presented in reference 4. The predicted thrust capability of a full scale design is also shown in Figure 18 from reference 9. The theoretical transition range utilizes dual blowing on the retreating blade and both a 1P and 2P cyclic control input. The RB-CCR model has by far exceeded the thrust capabilities that were predicted. Ultimately the aircraft concept would be compressor power or trim pressure limited but an aerodynamic thrust limit does not appear to be a constraint.

The effect of collective pitch angle on the unblown rotor will help explain the trim requirements and limitations in transition. Figure 19 presents the unblown characteristics of the RB-CCR model. The untrimmed pitching and rolling moment coefficient and the thrust coefficient for the transitional advance ratios are presented as a function of blade collective pitch angle. The magnitude of the untrimmed moments indirectly indicate the control power available from the RB-CCR concept. The untrimmed thrust curves establish an absolute minimum  $C_T/\sigma$  that the rotor model can obtain. This is particularly true for collective pitch angles which have zero or negative rolling moments. The lower collective pitch angles ( $-2^\circ$  to  $-4^\circ$ ) provide a much wider trim range but at a reduced rotor efficiency. The higher collective pitch angles ( $-1^\circ$  to  $+1^\circ$ ) provide optimum efficiencies but have a very limited thrust range and need much more flexibility in the control signal. One inference here is that a full scale rotor with an arbitrary pressure controller could operate with a fixed or zero collective pitch setting.

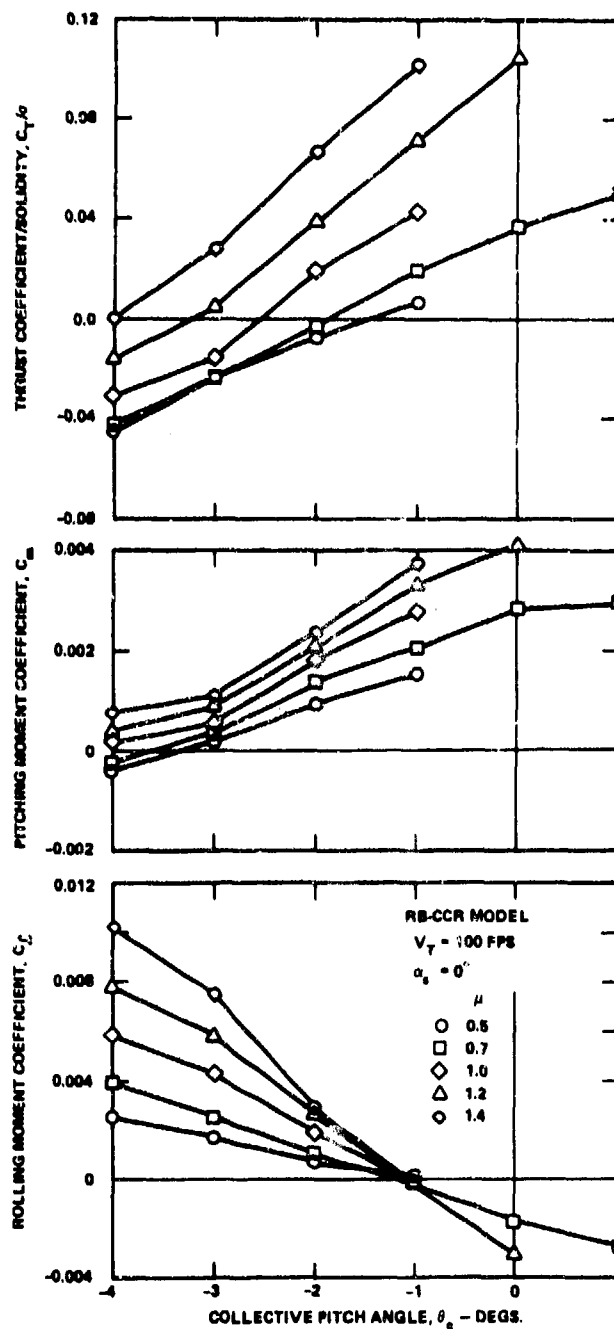


Figure 19 - RB-CCR Model Characteristics in Transition with No Blowing

## CRUISE

The third flight regime for the rotor is cruise which covers advance ratios of 1.4 to 4.0. The upper limit on advance ratio depends on the cruise velocity and how much the rotor can be slowed down (a dynamic/structural constraint). The cruise velocity depends on the aircraft drag and the amount of auxiliary power that is installed in the aircraft. Preliminary assessment of the cruise performance of the rotor was obtained. The rotor model was evaluated in a cruise configuration for advance ratios of 1 to 4. The purpose was to demonstrate the trim and thrust capabilities at high advance ratios and to ascertain the performance of the rotor; however, only a limited amount of data were obtained. One of the configurations evaluated was the same as that required in transition (i.e., dual blowing on the retreating side of the rotor and single blowing on the advancing side). The other configuration evaluated was alternate blowing between leading and trailing edge slots. The trailing edge slot was blown on the advancing side of the rotor ( $0^\circ < \psi < 180^\circ$ ) and the leading edge slot was blown on the retreating side ( $180^\circ < \psi < 360^\circ$ ). The latter configuration is envisioned for the RB-CCR concept. The 1P cam was used to differentiate blowing between the retreating and advancing sides of the rotor for both configurations. The cam was arbitrarily chosen and no attempt was made to optimize the cruise flight configurations. The effect of collective pitch angle on rotor trim and performance was determined. Because of the tunnel speed limitation, reduced tip speeds of 50 fps and 100 fps were required.

While dual slot blowing on the retreating side of the rotor does not limit the thrust capability, it does increase the compressor power which in cruise is almost all of the total power. A comparison of the two configurations shows that the total power for the alternate blowing scheme is approximately half the total power for the dual blowing scheme (Figure 20). The additional power for a collective angle of  $-4$  degrees is included. The total power is substantially more for  $\theta_c = -4^\circ$  than for  $\theta_c = 0^\circ$ ; but analysis of the data showed that the total power for  $\theta_c = 0^\circ$  and  $-2^\circ$  were about the same. This suggests that the rotor cruise efficiency is not very sensitive to collective pitch angle around zero degrees. The lifting system efficiency is presented in Figure 21 and shows that the model performs very well in cruise. The curves are loci of points indicating the best efficiency that was obtained with the model rotor. The data are not for optimum configurations but merely indicate the performance of the rotor in cruise. One of the limitations in running the cruise data was the tendency of the rotor to autorotate at relatively low blowing rates. When this happened, rotor rpm could not be held but would rapidly increase, at which time data taking had to be suspended. Figure 22 presents the rotor thrust coefficient at which autorotation begins (shaft power is zero) for advance ratios of 1 to 4.

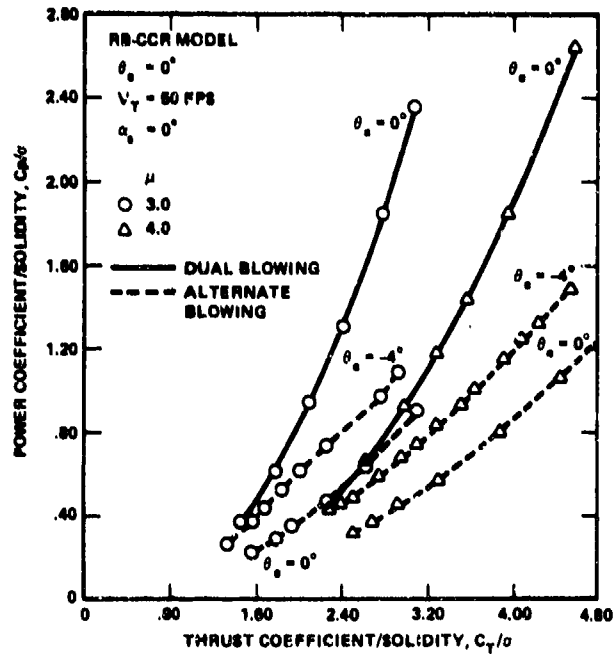


Figure 20 - Power Tradeoffs in Cruise

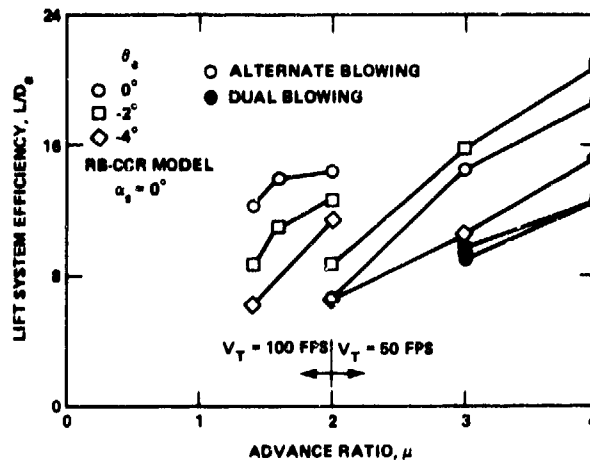


Figure 21 - Lift System Efficiency in Cruise

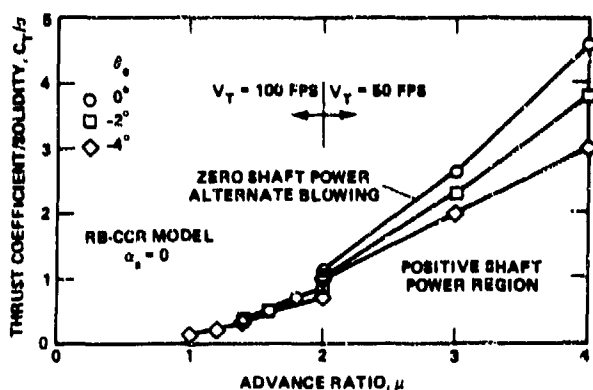


Figure 22 - Thrust Level For Autorotation in Cruise

### SUMMARY

The RB-CCR model has demonstrated that it is a viable high speed concept that merits further development. Any high speed rotor concept must have a low level of parasite drag in order to achieve acceptable aerodynamic efficiency in the cruise mode. Assuming such a reduction is feasible with the RB-CCR, the overall cruise efficiency will be quite high relative to today's helicopters. The RB-CCR model has demonstrated both the lift and trim capability needed to reduce rpm and transition to a high advance ratio cruise condition. Additional performance gains may be realized by going to shaft angles other than zero. There is an immediate need to obtain data at shaft angles other than zero before a shaft angle can be chosen for minimum power requirements.

The RB-CCR is not constrained to high solidity to go thru transition since blade loading can be raised by high section  $C_p$ 's which are characteristic of CC airfoils. Preliminary analyses show that relatively large sweep angles on the order of 45 degrees are not detrimental to augmentation and maximum lift coefficient of CC airfoils. Increased performance can be obtained by properly programming the control pressure signal.

The testing constraints placed on the model RB-CCR rotor at high advance ratio substantially limited its performance envelope. The model showed very strong tip speed effects, primarily Reynolds number phenomena, which are consistent with trends found in testing previous CCR models. The hover performance was considered to be very good for this (untwisted) rotor. The adverse effect of the open leading edge slot might be countered in a full scale design with a flexible slot lip.

In summary the RB-CCR model has validated the high speed circulation control concept. It has shown good performance in hover, very good thrust and trim capability in transition and has demonstrated high lifting system efficiency in cruise.

### REFERENCES

1. Smith, M.C.G., "The Aerodynamics of a Circulation-Controlled Rotor," 3rd CAL/AVLABS Symposium on Aerodynamics of Rotary Wing Aircraft, Buffalo, N.Y., Jun 1969.
2. Williams, R.M. and E.O. Rogers, "Design Considerations of Circulation Control Rotors," Paper 603, 28th National Annual Forum of the American Helicopter Society, Wash., D.C., May 1972.
3. Wilkerson, J.B., "Design and Performance Analysis of a Prototype Circulation Control Rotor," NSRDC Tech Note AL-290, Mar 1973.
4. Wilkerson, J.B. and D.W. Linck, "A Model Rotor Validation for the CCR Technology Demonstrator," Paper 902, 31st National Annual Forum of the American Helicopter Society, Wash., D.C., May 1975.
5. "Design Study of a Flight Worthy Circulation Control Rotor System," Kaman Aerospace Corporation Report R-1036-2, Contract N00019-73-C-0429, Jul 1974.
6. "Design Study of a Helicopter with a Circulation Control Rotor (CCR)," Lockheed Report LR26417, Contract N00019-73-C-0435, May 1974.
7. Williams, R.M., "Application of Circulation Control Rotor Technology to a Stopped Rotor Aircraft Design," Presented at the First European Rotorcraft and Powered Lift Aircraft Forum, Southampton, England, 22-24 Sep 1975.
8. Ottensoser, J., "Two-Dimensional Subsonic Evaluation of a 15-Percent Thick Circulation Control Airfoil with Slots at Both Leading and Trailing Edges," NSRDC Rpt 4456, Jul 1974.
9. Williams, R.M., "Recent Developments in Aerodynamics of Rotary Wings," AGARD-CP-111, Marseilles, France, 13-15 Sep 1972.
10. Montana, P.S., "Experimental Investigation of Three Rotor Hub Fairing Shapes," NSRDC, ASED Report 333, May 1972.
11. Reader, K.R., "Control System for a Reverse Blowing Circulation Control Rotor (RB-CCR) Wind Tunnel Model," NSRDC Rpt 76-0062, Apr 1976.

## INITIAL DISTRIBUTION

**Copies**

1 AMC/AMCRD-FA  
 1 ARO/Engr Sci Div  
     S. Kumar, Asso Dir  
 1 AASC/Lib  
 1 AAMCA/AMXAM-SM  
 2 AAMRDL/Ft. Eustis  
     1 Lib  
     1 SAVRE-AM  
 2 AAMRDL/Ames Res Cen  
     1 Tech Dir  
     1 A. Kerr  
 1 CMC/Sci Advisor  
     A.L. Slafkosky  
 1 ONR/Aeronautics, Code 461  
 2 NRL  
     1 Tech Info Office  
     1 Lib, Code 2029  
 1 USNA  
 2 NAVPSCOL  
     1 J. Miller/Aero-Engr  
     1 L. Schmidt  
 4 NAVAIRDEVGEN  
     1 Tech Dir  
     1 Tech Lib  
     1 R. McGiboney  
     1 G. Woods  
 17 NAVAIRSYSCOM  
     1 AIR 03  
     1 AIR 03PA (W. Koven)  
     1 AIR 03B (F. Tanczos)  
     1 AIR 03P  
     CAPT von Gerichten  
     2 AIR 320D (R. Siewert)  
     4 AIR 320B (A. Somoroff)  
     1 AIR 5104

**Copies**

NAVAIRSYSCOM (Continued)  
 1 AIR 530B (H. Andrews)  
 1 AIR 530214A (R. Malatino)  
 1 AIR 530112 (R. Tracey)  
 1 AIR 530311 (F. Paglianete)  
 1 AIR 604  
 1 AIR PMA-247  
     CDR Friichtanicht  
 2 NAVAIRTESTCEN  
     1 Dir, TPS  
     1 N. Jubeck  
 12 DDC  
 1 AF Dep Chief of Staff  
     AFRDT-EX  
 2 AFFDL  
     1 FDV, VTOL Tech Div  
     1 FDMM, Aeromech Br  
 1 AFOSR/Mechanics Div  
 1 FAA, Code DS-22  
     V/STOL Programs  
 3 NASA HQ  
     1 A. Evans  
     1 A. Gessow  
     1 J. Ward (MS-85)  
 6 NASA Ames Res Cen  
     1 Tech Lib  
     1 Full-Scale Res Div  
     1 M. Kelley/Lg-Scale Aero Br  
     1 R.T. Jones  
     1 J. McCloud  
     1 J. Rabbot  
 4 NASA Langley Res Cen  
     1 Tech Lib  
     1 R. Huston  
     1 L. Jenkins  
     1 R. Tapscott  
 1 Va Polytechnic Inst/Dept Engr Mech  
     D.T. Mook

Copies

2 West Va U/Dept Aero Engr  
1 J. Fannuci  
1 J. Loth

1 Analytical Methods/F. Dvorak

1 Bell Aerospace Corp/Ft. Worth Lib

2 Boeing Co/Seattle  
1 Tech Lib  
1 P.E. Ruppert

2 Boeing Co/Vertol Div  
1 Tech Lib  
1 W.Z. Stepniewski

1 Fairchild-Hiller/Farmingdale  
1 Republic Aviation Div

1 Gen Dyn/Convair Div  
Tech Lib

1 Grumman Aerospace Corp  
M. Siegel

2 Honeywell, Inc/S&R Div  
1 Tech Lib  
1 R. Rose

2 Hughes Tool Co/Culver City  
1 E. Wood  
1 A/C Div

3 Kaman Aerospace Corp  
1 Tech Lib  
1 D. Barnes  
1 A. Lemnios

1 Ling-Temco-Vought, Inc/Lib

4 Lockheed A/C Corp/Burbank  
1 Tech Lib  
1 P. Kesling  
1 E. Martin  
1 B.R. Rich

1 Lockheed-Georgia Corp/Lib

1 McDonnell-Douglas/Long Be  
T. Cebeci

1 Northrop Corp/Hawthorne Lib

Copies

1 Paragon Pacific Inc.  
J.H. Hoffman

1 Piasecki Aircraft Corp

1 Rochester Appl Sci Asso, Inc/Lib

2 Teledyne Ryan Aeronautical  
1 P.F. Girard  
1 Lib

1 United A/C Corp/E. Hartford

3 United A/C Corp/Sikorsky  
1 Lib  
1 T. Carter  
1 I. Fradenburgh

1 Vizex, Inc/R.A. Piziali

#### CENTER DISTRIBUTION

Copies	Code
30	5214.1 Reports Distribution
1	522.1 Library (C)
1	522.2 Library (A)
2	522.3 Aerodynamics Library

**DTNSRDC ISSUES THREE TYPES OF REPORTS**

(1) DTNSRDC REPORTS, A FORMAL SERIES PUBLISHING INFORMATION OF PERMANENT TECHNICAL VALUE, DESIGNATED BY A SERIAL REPORT NUMBER.

(2) DEPARTMENTAL REPORTS, A SEMIFORMAL SERIES, RECORDING INFORMATION OF A PRELIMINARY OR TEMPORARY NATURE, OR OF LIMITED INTEREST OR SIGNIFICANCE, CARRYING A DEPARTMENTAL ALPHANUMERIC IDENTIFICATION.

(3) TECHNICAL MEMORANDA, AN INFORMAL SERIES, USUALLY INTERNAL WORKING PAPERS OR DIRECT REPORTS TO SPONSORS, NUMBERED AS TM SERIES REPORTS; NOT FOR GENERAL DISTRIBUTION.